Proceedings of the 2nd Marine Energy Technology Symposium
METS2014
April 15-18, 2014, Seattle, WA

DESIGN AND INITIAL COMPONENT TESTS OF AN INTEGRATED AVIAN AND BAT COLLISION DETECTION SYSTEM FOR OFFSHORE WIND TURBINES

Jeremy Flowers
School of Mechanical, Industrial & Manufacturing Engineering
Oregon State University
Corvallis, OR, U.S.A.

Roberto Albertani
School of Mechanical, Industrial & Manufacturing Engineering
Oregon State University
Corvallis, OR, U.S.A.

Trevor Harrison
Northwest National Marine Renewable Energy Center
University of Washington
Seattle, WA, U.S.A.

Brian Polagye
Northwest National Marine Renewable Energy Center
University of Washington
Seattle, WA, U.S.A.

Robert M. Suryan
Oregon State University
Hatfield Marine Science Center
Newport, OR, U.S.A.
rob.suryan@oregonstate.edu

ABSTRACT

We describe the development and initial testing of a multi-sensor instrumentation package capable of detecting avian and bat interactions with offshore wind turbines. The system design emphasizes the ability to detect collisions with the blades, tower, and nacelle of a turbine and to provide taxonomic classification of the animal involved in the collision. This system will allow the environmental impacts of offshore wind turbines to be remotely monitored and help ensure that the benefits of renewable power generation are not outweighed by mortality of protected species. Conceptual design of the complete system, initial testing of vibration sensors, and proof of concept for sensor integration and event detection are presented.

INTRODUCTION

Offshore wind is expected to play a significant role in reaching targets for 20% of United States electricity generation to come from wind resources by 2030 [1]. The installation of between 50 and 90 GW of offshore wind capacity will require an investment of over $200 billion for construction, operation, and infrastructure development (e.g. crane vessels for offshore wind turbine installation and repair) [1]. However, it is imperative that this development not impact avian and bat species, particularly those that are threatened or endangered. This risk can be mitigated through environmental impact assessments prior to installation and monitoring programs once projects are in operation. While onshore wind energy projects are subject to similar scrutiny, established methodologies for assessing mortality of avian species through carcass collection [2] are infeasible in the offshore environment. Consequently, for offshore wind to realize its renewable generation potential without impacting volant species, new and economical approaches to environmental monitoring are required. Such approaches should be able to automatically detect aerial targets near a turbine and collisions with the turbine, as well as provide information for subsequent taxonomic identification (e.g., animal size, coloring, wing beat frequency, vocalization/echolocation). This paper describes the development of a multi-sensor package that integrates temporal and spatial coverage capacities to optimize detection of collision/strike events and characterize the avian and bat species in close proximity to offshore wind turbines.

Offshore Wind Development

The electrical capacity of offshore wind turbines continues to increase with each generation of technology. For example, the Siemens SWT-6.0-154 (6 MW) offshore wind turbine has blades that are 75 m long and a hub that is 4 m in diameter. Hub height is selected in a site-specific manner, but often more than a hundred meters above sea level. Larger turbines, with capacities approaching 10 MW are under development.

The siting of terrestrial wind facilities has greatly influenced the extent of bird and bat impact

mortality, and similar concerns exist in the placement of offshore renewable energy facilities. Areas of high animal density, low density, and migration corridors occur over certain areas, often associated with key marine habitat features such as water depth, shoreline topography, and distance to shore [3]. For example, along the U.S. west coast, the inner continental shelf bird community is dominated by heavy bodied diving species with relatively low flight heights (often < 10 m), whereas the outer shelf-slope and offshore communities are dominated by surface feeding and dynamic soaring species with greater flight heights (10s–100s m) [3,4]. Such flight behavior greatly influences potential interactions with different renewable energy devices (e.g., wave vs. wind).

For wind turbines deployed on the west coast of the United States, two signature avian species of regulatory concern include the marbled murrelet (*Brachyramphus marmoratus*) and the short-tailed albatross (*Phoebastria albatrus*). These two species reflect a wide variety in body size for birds found offshore: a body length of 24 cm and mass of 202 g for the murrelet to 91 cm and 4,680 g for the albatross. Both species can fly at speeds up to 26 m/s (94 km/h) or more. Their morphology and flight behavior are also quite different with marbled murrlets being a diving species with small wings that typically fly close to the surface of the water, whereas albatrosses exhibit dynamic soaring during which they arc high above the water's surface with large, extended wings (2.3 m), thereby influencing the types of renewable energy devices and which part of the structure each bird would most likely encounter. The likely bat species that could occur off the west coast are the hoary (*Lasiurus cinereus*) and silver-haired (*L. noctivagans*) bats. With body sizes ranging from 11-15 cm and 10-30 g, these bats are comparable in size to the smallest marine birds, but considerably smaller than most marine birds.

Body mass and flight speed will affect both the impact kinetics and the frame rate necessary for cameras to catch multiple images of the bird or bat for identification as it passes through the camera's field of view. Whereas the impact kinetics with a fixed structure is a function of mass and speed of the animal, the magnitude of an impact with a wind turbine blade will likely most often be a function of the animal mass and the blade speed (i.e., rpm and distance from the blade root) - it is more likely that a bird would be hit by the leading edge of a blade than the animal running into the rapidly moving face of the blade (up to 250 km/hr or more). Therefore, during our experimental impact testing of the sensor array, we vary the mass of the object impacting the blade, but not the speed at which it is launched.

Prior Research and Development

One approach for automatic detection of avian and bat collision with wind turbines is vibrational or acoustic sensing devices. Wiggelinkhuizen et al. [5] developed the WT-Bird bird collision monitoring system. The system initially employed wired contact microphones (piezoelectric transducers sensitive to sound propagating through solid structures) on the blades before switching to wired accelerometers to improve durability and signal-to-noise ratios. This work indicated that it should be feasible to detect strike events from the resulting structural vibration.

A second approach is the use of camera systems, either in the visual- or infrared-spectrum. While visual camera imagery is more effective for species identification because of high pixel resolution and color contrast, infrared (IR) systems are able to operate over a broader range of environmental conditions (e.g., operation at night). One notable IR system is Desholm et al.'s [6] Thermal Animal Detection System (TADS), which achieved taxonomic classification through wing beat analysis and animal size, in addition to detection. Detection and identification functions were not automated and required manual review of imagery collected on a pre-determined duty cycle [6]. A more targeted approach was used by the WT-Bird system, whereby the vibration sensors triggered the visual cameras, recording only imagery of greatest interest. The WT-Bird positioned two visual cameras on the tower base looking upward. In this configuration they were able to monitor approximately 90% of the rotor swept area [5].

Multi-Sensor Detection Package with Event-Based Data Collection

Recognizing the benefits of a multi-sensor approach from both the TADS and WT-Bird system, an integrated sensor package is being developed around five fundamental sensor types:

- accelerometers (wireless)
- contact microphones (wireless)
- visual cameras (cabled)
- infrared (IR) cameras (cabled)
- bioacoustic microphones (cabled).

The system consists of multi-sensor nodes communicating with a central controller and data acquisition system.

The vibration sensors (accelerometers and contact microphones) provide continuous temporal coverage for collision detection. The central challenges associated with these sensors are filtering strike events from routine vibration and ensuring wireless connectivity with the

controller. Wireless connectivity and on-board battery power allow these sensors to be installed on existing turbines with minimal impact.

The optical systems, consisting of visual and IR cameras, provide the necessary information for taxonomic classification, as well as gathering information on presence and near misses. While visual cameras provide the most comprehensive taxonomic information, they are limited to daytime use. IR cameras are effective in a broader range of environmental conditions and provide higher contrast imagery for target detection, but have limited resolution and higher cost than visual-spectrum cameras. The central challenges associated with the optical systems are data bandwidth and storage, real-time image processing for trigger events, and limits in spatial coverage imposed by the field of view and cost of each instrument.

The sensor system also includes passive bioacoustic recording for temporally and spatially continuous detection of bat presence and taxonomic classification. This system will communicate with the central controller and be retained within the ring buffer described below to be transmitted with all other strike event detection data. Bioacoustic signal reception, however, is currently not included in automated detection algorithm development and is not discussed in detail in this paper. Adapting a bioacoustic triggering algorithm and passive acoustic detection of seabirds is being considered for future inclusion in the instrumentation package.

In summary, each of these sensors has capabilities that may include detection of presence, detection of collision/impact, and taxonomic classification. Similarly, spatial coverage for individual instruments ranges from omnidirectional (e.g., bioacoustics) to narrow fields of view (e.g., high-resolution IR camera) and temporal availability ranges from continuous (e.g., accelerometer) to limited (e.g., visual camera). Consequently, an instrumentation package which detects collisions and identifies the avian or bat species involved requires a multi-sensor, multi-node solution.

Prior studies indicate that collision rates with offshore wind turbines are low [6] and continuous data collection may be required to capture rare events. However, continuous acquisition of visual imagery is of high enough bandwidth to preclude archival of all imagery (e.g., data rates from a single visual-IR camera node approach 1 Gbps). This limitation is overcome through an event-based triggering architecture that addresses storage issues associated with long term deployment and reduces the volume of data requiring post-processing or manual review.

METHODS

Accelerometers and Contact Microphones

Vibration Signal Processing by Wavelet Analysis

Wavelet analysis is a powerful tool for joint analysis of time and frequency domains. Applications include operation and maintenance, media and image file compression, and engine knock detection [7-9]. In our case, wavelet analysis is implemented to distinguish collision events from routine vibration. Wavelet analysis decomposes the signal of interest into sinusoids. Convolution is then performed by comparing a "mother" wavelet with the decomposed signal. A mother wavelet is a wave shaped oscillation that begins and ends at zero amplitude. A preliminary search has been performed to find a suitable mother wavelet for this application. Currently, a Coiflets 5 mother wavelet (impulsive signal) is being used. Using this mother wavelet, multiple convolution passes are performed on the signal. The results are improved by adjusting the scaling function and the mother wavelet during each analysis pass. A significant benefit to wavelet analysis is that it can be performed in real time [7,10].

Laboratory Testing

Before deployment on a wind turbine, preliminary evaluation and verification of wavelet analysis on accelerometers (LORD MicroStrain G-Link LXRS w/ 104-LXRS base station) and contact microphone (Sun-Mechatronics USK-40 w/ UZ-10 UHF receiver) signals were performed in the lab. The accelerometer signal is digitized prior to wireless transmission, while the contact microphone signal is transmitted as an analogue signal. The contact microphone signal was digitized by a NI USB-4431 DAQ (www.ni.com).

In the laboratory, we generated simulated data that included a sine wave interspersed with impact events (impulsive transients) to simulate an event masked by background vibration. This synthetic time series was used to select the candidate mother wavelet described above. Further laboratory evaluation involved data collection from an accelerometer and a contact microphone attached to a programmable shaker table. During the recording, "impact" events were created by tapping the shaker table. For these experiments, the sampling rate was 512 Hz for accelerometers and 1000 Hz for microphones.

In addition to sensor function, laboratory studies also evaluated wireless connectivity. These tests involved quantification of the sensor transmission range in the presence of interference similar to that expected in the field.

Field Testing

The first phase of this system's field testing was performed at the North American Wind

Research and Training Center (NAWRTC) at Mesalands Community College in Tucumcari, New Mexico. One wireless accelerometer and one wireless contact microphone were mounted to the root of each blade of the facilities 1.5 MW GE wind turbine as shown in Figure 1.

FIGURE 1: (L) THE NAWRTC WIND TURBINE (R) ATTACHMENT CONFIRGURATION FOR THE SENSORS ON THE BLADE

The wireless receivers and a data acquisition computer were placed about 80 m upwind from the base of the tower. In operation, the receivers and data acquisition hardware would be housed within the turbine nacelle. Since bird collisions are rare, testing required generating prototypical impact events. Developers of the WT-Bird system found sand bags [11] and weighted tennis balls launched with a "gas-pressurized launcher" effective at generating impact events [5]. Following this methodology, a compressed-air cannon was constructed for the launching of tennis balls to create strike events at the blades. Tennis balls (~57 g) empty and filled with water (~140 g) were used in the testing to represent some of the smallest marine birds and only twice the mass of the largest bat likely encountered. The tennis balls were launched from the ground about 10 m downwind of the plane of the blades in an upwind direction, providing two potential passes through the rotor swept area per launch when the wind velocity was sufficiently high - one pass traveling upwind and if not struck by a blade, then a second pass if the ball was blown back downwind through the rotor swept area.. The accelerometer and contact microphone acquired data continuously at 512 and 1000 Hz, respectively. Vibration data were also recorded during start up, shut down, generator engagement, pitching/yawing actions to evaluate the potential to detect collisions during transient operational states.

Visual and Infrared Cameras

Configuration of Optical Systems

Unlike vibration sensors, optical systems may be able to not only detect collisions, but also provide information allowing taxonomic classification of the animal involved. There are several options for mounting optical systems, each involving a trade-off between field of view and complexity of automated image processing. For reasons of cost, any practical camera implementation will involve incomplete spatial coverage. Optical cameras could be deployed in one of five configurations:

- On the nacelle, with a field of view that does not intersect the rotor plane (in a downward configuration, the view would also include the tower).
- On the nacelle, with a field of view that intersects the rotor plane (i.e., blade passage is observed by the camera).
- On the turbine tower, near its base, in an upward facing configuration.
- On the root of the blade, with a field of view that includes most of one side of a blade.
- On an adjacent tower viewing entire rotor swept area.

Cameras mounted on the nacelle will yaw with the rotor plane, while cameras on the turbine tower will not track the rotor plane without additional mechanisms. A camera mounted on an adjacent tower would provide superior spatial coverage, but at the cost of diminished resolution that would limit detection of presence and collision to the largest seabirds. Consequently, the latter option is not discussed at length.

For a camera deployed on the nacelle with a field of view excluding the rotor, automated image processing to detect animal presence is most straightforward. Potential false positive targets include insects, waves (for cameras with a field of the view including the water surface), and clouds (for cameras with a field of view including the sky). However, observations of collision in the rotor plane are unlikely, since an animal approaching from the upwind side of the turbine would be unlikely to be projected into a downwind camera's field of view if struck by a blade. Cameras in this configuration could, however, observe animals that have passed through the rotor swept area without a collision and could also observe collision with the tower.

If a camera is deployed on the nacelle with a field of view intersecting the rotor plane, image processing would be somewhat more difficult since additional false positive images would also be created by the passage of the turbine blades (high contrast with background). However, image processing algorithms should be capable of "subtracting" the blades or rejecting them on the basis of target size. In this orientation, direct observations of collision/strike are possible, though the leading edge of the blade may be obscured by the body of the blade.

Cameras deployed at the base of the tower would be able to observe collision with the tower,

as well as strike/collision over the lower half of the rotor swept area. However, a camera in this orientation will not automatically yaw with the rotor plane (as would a camera on the nacelle). Cameras in this configuration would be subjected to rain and debris from above and to salt spray on a more regular basis than those on the nacelle and, consequently, at greater risk of corrosion and fouling. These are significant limitations. Image processing complexity is slightly reduced since false positive detections from wave action are not possible.

Cameras deployed on the suction side of the blade root offer the least hardware intensive solution for capturing collision events, with only one camera node required to provide complete spatial and temporal coverage per blade. Integration of the cameras with the turbine would be substantially more complicated in this scenario: cameras would be more difficult to physically install, system maintenance would be difficult, communication with the control system in the nacelle would require high-bandwidth wireless connectivity, and power would need to be provided via a slip ring. While false positive detections associated with blade motion are unlikely for automated processing, algorithm complexity is elevated due to the continuously varying background.

While blade root mounting is conceptually attractive, the complexity of deployment and image processing is high enough to recommend that, for first-generation systems, only a portion of the rotor swept area should be observed from a fixed package on the nacelle with a field of view including the turbine rotor. If impacts are equally likely throughout the rotor swept area, then cameras would be best positioned viewing down from the sides or underside of the nacelle such that it would be possible to simultaneously observe tower collision. For installation simplicity in initial field testing, the prototype camera node will be mounted to the upper nacelle, with a field of view intersecting the rotor swept area.

Considerations for Hardware Selection

Hardware selection for the optical sensors (visual and infrared) is driven by image resolution (the product of target size/distance, sensor resolution, and field of view) and depth of field (i.e, the region of the field of view that is in focus). In general, the depth of field is related to the field of view and lenses with a wide field of view often also have a large depth of field. Species distinction between two small similar birds, such as a Cassin's auklet (*Ptychoramphus aleuticus*) and a marbled murrelet, will be difficult if the bird is represented by only a few pixels within the image. Determining the spatial resolution of an object (in number of pixels) at a given distance allows a user to determine the practical range for identification. Neglecting lens distortion, at a given distance (D) from the camera, the width (L) of the field of view is given as a function of the lens angle (θ) by the trigonometric relation

$$L = 2D\tan\left(\frac{\theta}{2}\right).$$

The size of a pixel at distance D is then given as L/R_x, where R_x is the horizontal resolution (i.e., 640 pixels). The number of pixels spanning a target of interest, such as a marbled murrelet, can then be readily calculated on the basis of estimated body size. Target detection is unlikely to be possible if there are less than 3-4 pixels spanning a target. Figure 2 shows the results of this thought exercise for an infrared camera with a 640x480 pixel resolution and two different lenses installed in an upward facing configuration on the nacelle of a Siemens SWT-6.0-154. While target detection is likely to be possible over the entire blade span for the narrow field of view camera, spatial coverage is poor. Conversely, a lens that nominally provides a wider field of view is unlikely to allow target detection over more than half of the blade span.

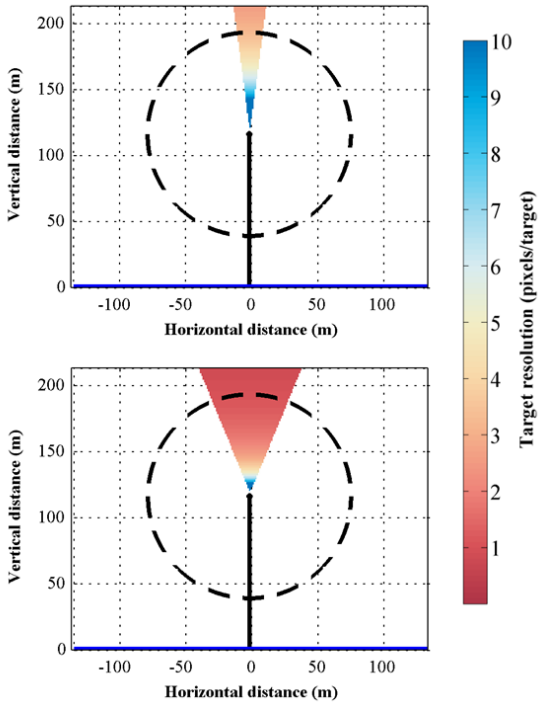

FIGURE 2: TARGET RESOLUTION (PIXELS/TARGET) FOR A MARBLED MURRELET PASSING THROUGH THE FIELD OF VIEW FOR A 640 X 480 INFRARED CAMERA. (T) 15⁰ FIELD OF VIEW LENS (B) 45⁰ FIELD OF VIEW LENS. DASHED LINES CORRESPOND TO EXTENT OF ROTOR SWEPT AREA.

Particularly for IR cameras, image resolution may be insufficient for taxonomic classification of targets. One approach to provide additional

information is the use of camera pairs at a fixed baseline separation and orientation to produce stereo imagery. A calibrated stereo camera can be used to determine the size and three-dimensional location of targets in space. This is a powerful capability for distinguishing collisions from near misses, as well as providing information about body length and flight speed for taxonomic classification. This capability is being developed for both the infrared and visual spectrum cameras in the instrumentation package.

The current generation of uncooled microbolometer-based IR cameras have a maximum resolution of 640x480 (0.3 Megapixel – Mpx). For proof of concept testing, a pair of FLIR A655sc cameras (www.flir.com) were selected. These cameras have 640x480 resolution, can acquire visual imagery at 50 frames per second (fps), and are compatible with the GigE Vision standard.

Machine vision optical cameras have much higher resolution, in some cases exceeding 10 Mpx. The visual-spectrum stereo camera pair utilized in this project are Allied Vision Technology Manta 201-C units (www.alliedvisiontec.com). These cameras have 2 Mpx resolution, can acquire imagery at up to 14 fps, and are compatible with the GigE Vision standard. In addition, "smart" cameras with onboard image processing capabilities are being considered to reduce network traffic and the processing load on the central controller. One example under evaluation, is the Ximea Currera-RL50C (www.ximea.com), which can record at 15 fps at a resolution of 5 Mpx and includes a Gigabit Ethernet network interface card (NIC).

Both the IR and visual-spectrum cameras can communicate with each other and the central controller over a Gigabit Ethernet network (maximum bandwidth 1 Gbps). This common communication basis simplifies integration of hardware in the optical node.

Automated Target Detection

Automated target detection in the visual spectrum is difficult to achieve in real time because the computational requirements for image processing. Targets in the infrared spectrum, however, often have high contrast relative to their background and, consequently, simple contrast threshold algorithms can be used to detect targets that move quickly relative to the background. A basic detection algorithm is, as follows:

1. Calculate a "mean" image based on *N* frames surrounding the image in which target detection is required. Algorithm sensitivity increases with *N* (desirable), as do the number of false positive detections (undesirable).
2. Subtract the frame of interest from the mean image.
3. Convert the result to a binary image based on a minimum threshold contrast difference between the image of interest and the mean. Algorithm sensitivity increases with a lower contrast threshold.
4. Identify regions of the binary image with multiple connected "positive" pixels.

By repeating the above process for multiple frames, detected targets can be tracked. Further processing of sequential images can reduce false positives by eliminating targets without a continuous trajectory. The primary challenge to this detection algorithm is appropriate selection of *N* and the contrast threshold for binary image generation.

Algorithm proof of concept was established using avian imagery collected in the field by the IR camera at 25 fps. The algorithm described above was implemented in Matlab (www.mathworks.com) using the functions included in the Image Processing Toolbox.

Event-Based Trigger Architecture

For a single camera node with stereo image capability in the infrared and visual spectra, continuous acquisition at frame rates sufficient to capture fast moving targets will produce tens of terrabytes of data per day. This is a prohibitory volume of data to be archived for post-processing. To address this challenge, an event-driven storage architecture has been developed. Each sensor connected to central controller continuously streams data into a circular buffer (ring buffer) which holds a user-defined temporal window of data in temporary storage. If an event (detection or collision) is registered by any sensor channel, a copy of the data from all buffers will be made following a time delay of half the window size (i.e., equal data acquired on both sides of an event). This copy of buffered data may then be asynchronously written to disk, limiting the potential for gaps between sequential event detections. This architecture minimizes the volume of "non-event" data archived and computational expense for post-processing. The data structure also accommodates sensor specific and cross-sensor event registration algorithms which eases development of low false positive triggering (i.e., buffer archival without an actual collision or presence) and zero false negative triggering (i.e., no buffer archival following an actual collision) required for automated remote sensing systems. For example, while initial testing will allow any sensor with automatic detection capabilities to "raise" an event, subsequent refinement may require multiple

sensors to raise an event to limit the number of false positives. Archived data will then be transmitted back to shore for additional post-processing and review for species identification.

Proof of concept architecture has been implemented in LabView (www.ni.com/labview) and tested in the laboratory with a pair of IR camera streams and manual event triggering. These tests utilized a customized Clevo W650SR laptop computer (www.pro-star.com) with the following specifications: one 256 GB SSD for the operating system, two 1 TB spinning hard disks for data storage, and 16 GB RAM. The computer is capable of managing the bandwidth and memory of a single, prototype optical node, composed of two visual and two IR cameras. For a system deployed on a commercial turbine, the acquisition system would require a server with one network interface card per optical node.

RESULTS

Laboratory Tests of Accelerometer and Contact Microphones

Figure 33 (T) shows a representative sequence of a raw data from the wireless accelerometer attached to the shaker table. The wavelet processing allows the tapping instances to be more clearly identified against the background vibration, as shown in Figure 33 (B).

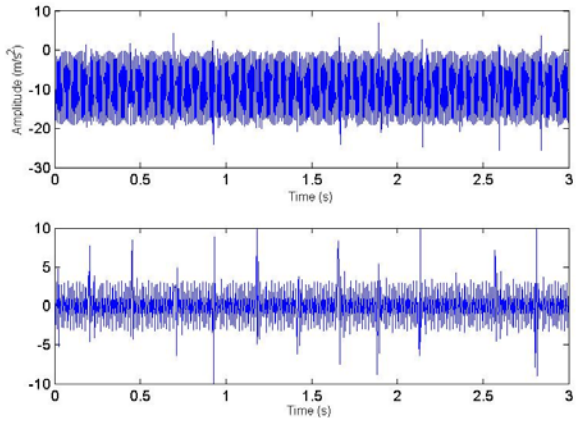

FIGURE 3: (T) RAW SIGNAL FROM ACCELEROMETER ATTACHED TO SHAKER WITH IRREGULAR TAPPING TO SIMULATE IMPACTS (B) WAVELET ANALYSIS HIGHLIGHTING IMPACT SIGNALS

Field Tests of Accelerometer and Contact Microphones

Although the data collected from the sensors at NAWRTC has not been thoroughly evaluated, some interesting preliminary observations of event detection and sensor tendencies are possible. For both the accelerometer and contract microphone line of sight clarity to the receiver had a significant effect on wireless transmission range. During our testing, the wireless receiver was at ground level, 80 m from the sensors attached to the root of each of the 3 blades. Manufacture specified wireless transmission distance of digital, accelerometer data was a maximum of 2 km line of sight with the use of the extended range setting. At 80 meters distance with the blade motion, we experienced some reception failure, especially at slow blade rotation speed, but fortunately the accelerometers were designed to store and resend data packets that were not successfully transmitted. We, therefore, experienced negligible accelerometer data loss. Manufacture specified wireless transmission distance of analog contact microphone data was shorter (80 - 150m line of sight) than accelerometers, appeared more affected by blade orientation, and did not store data packets for repeated transmission like that of digital data. However, under normal operation there was sufficient communication between wireless microphones and the receiver for accurate data collection. Unfortunately, the contact microphones flagged one false event every second during certain wind conditions, which will require further algorithm development to prevent. The strong signal generated by turbine shutdown, pictured in Figure 4, also indicates the necessity for filtering false positive events from the microphone signal (Figure 4T). Intentional impacts from both the weighted and un-weighted tennis balls created strong observable events along the blade span, with impacts at the blade tip consistently producing strong signals. Further work is underway to perform wavelet analysis on visually undetectable events.

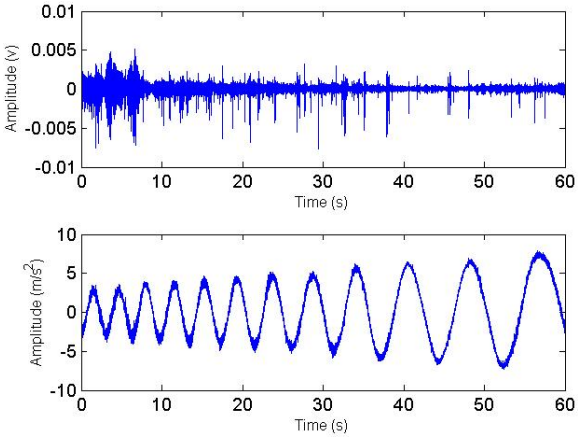

FIGURE 4: REPRESENTATIVE TURBINE SHUTDOWN MEASUREMENTS FOR A MICROPHONE-ACCELEROMETER PAIR ON THE SAME BLADE, MICROPHONE (T), ACCELEROMETER (B)

Figure shows time series measurements for all six sensors (one accelerometer-microphone pair

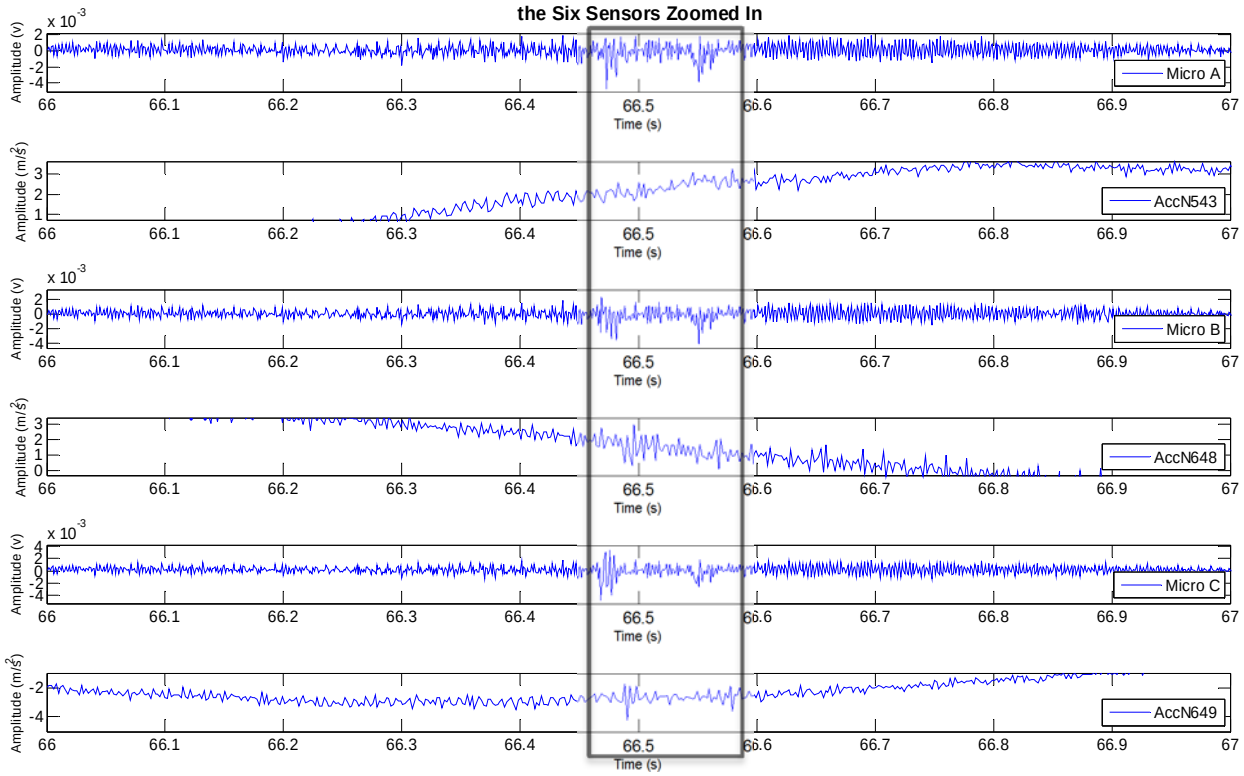

FIGURE 5: MEASURED EVENT REACTION (BOXED) FOR ALL THREE ACCELEROMETER-MICROPHONE PAIRS

per blade) during an impact on one blade. The impact is visually apparent in the signals from all three microphones and on two of the accelerometers (N648 and N649). Based on the magnitude of the signal, it is most likely that the impact occurred on the blade with sensor pair Micro C-N649.

Automated Target Detection

Proof of concept for the automated targeted detection algorithm for the infrared camera is demonstrated by the sequence shown in Figure . For this sequence, a single bird is detected against slowly moving clouds in infrared imagery recorded at 25 fps. Ten frames to either side of the frame of interest (±0.4 s) are used to construct the mean image and a threshold intensity of 60 (out of 255) is used to produce the binary image. The cloud is nearly the same temperature as the bird, but moves more slowly through the field of view and, consequently, produces less contrast in the background-subtracted image. Residual clutter associated with both the bird's flight path and cloud motion is removed by the binary image threshold. While target identification (as a bird) is straightforward in the video sequence, the limited resolution of infrared cameras is apparent in the individual frame shown in Figure .

Event-Based Triggering

Initial lab testing of the LabView event-based data collection program has provided some first order measures of memory and network bandwidth requirements. Simultaneously streaming images from the two FLIR A655sc cameras at their maximum frame rate of 50 Hz into a 10 second circular buffer (± 5 seconds centered around event), for a total of 1000 images in temporary storage, requires only 0.8 GB memory. The current version of the program archives buffer data following input of a manual trigger, pausing the monitoring stream for 2-3 seconds while the entire image buffer (1000 x 0.7 MB per image) is written to hard drive in TIF format. While this pause is brief, continuous capacity is preferable and will be achieved with an asynchronous write to disk. The next software iteration will also incorporate automatic triggering by component sensors.

As anticipated, the data stream does require approximately half the bandwidth (480 Mbps) of the 1Gb Ethernet network connection. While the visual cameras have a lower maximum frame rate, this is offset by a higher resolution and they will saturate the network connection. This bottleneck will inform the optimization of acquisition settings for field testing.

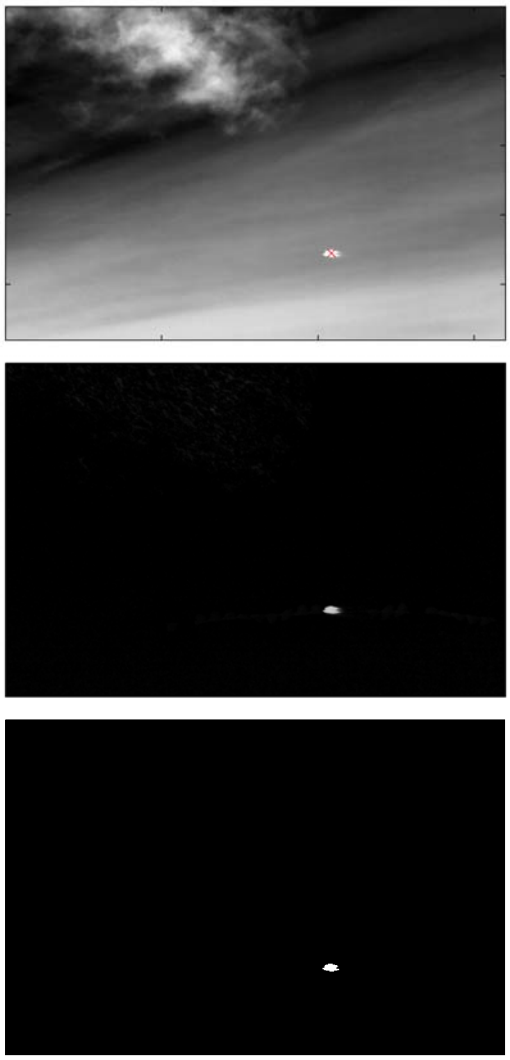

FIGURE 6: PROOF OF CONCEPT FOR AUTOMATED IR CAMERA TARGET DETECTION. FROM TOP TO BOTTOM: RECORDED IMAGE (X MARKS TARGET), IMAGE WITH MEAN REMOVED, BINARY THRESHOLDED IMAGE.

DISCUSSION

The need for integrated instrumentation packages for environmental monitoring are not limited to wind energy [12-14]. A recent expert workshop [15] discussed monitoring needs for wave and tidal energy converters and reached similar conclusions.

In addition to environmental monitoring, the data collected by contact microphones and accelerometers could support condition health monitoring of offshore wind turbine structures. Considering both blade and blade tip failures, a wind turbine may need to be serviced 0.44 times a year just for blade related failures out of a total of 2.20 estimated yearly failures [16]. Offshore wind turbine repairs are 5-10 times more costly to perform than their onshore counterpart due to weather scheduling delays and the vessel mobilization costs [16-17]. Vibration sensors can play a role in preventative maintenance by limiting the number and cost of unplanned interventions. Other studies have identified wireless accelerometers mounted to wind turbine blades as a tool to detect blade damage [18-19].

CONCLUSION

Low-cost approaches to remote monitoring of avian and bat interactions with offshore wind turbines are needed to reduce market barriers to deployment. This paper describes the development and initial testing of a multi-sensor instrumentation package that includes both vibration sensors and optical cameras networked together in an event-triggered data acquisition system. Field testing of the complete system is planned for fall 2014 at the National Renewable Energy Laboratory's National Wind Technology Center.

ACKNOWLEDGEMENT

The authors wish to acknowledge the financial support of the US Department of Energy under DE-EE0005363. We are grateful for assistance from the North American Wind Research and Training Center's staff at Mesalands Community College in making the system's first field test successful. The authors also wish to thank staff and scientists at NREL for their willingness to share information with the team and use of the Controls Advanced Research Turbines at the National Wind Technology Center for system testing and demonstration. Finally, we greatly appreciate the review and expert contribution of our science and industry advisory panel.

DISCLAIMER

This report was prepared as an account of work sponsored by an agency of the United States Government. Neither the United States Government nor any agency thereof, nor any of their employees, makes any warranty, expressed or implied, or assumes any legal liability or responsibility for the accuracy, completeness, or usefulness of any information, apparatus, product, or process disclosed, or represents that is use would not infringe privately owned rights. Reference herein to any specific commercial product, process, or service by trade name, trademark, manufacturer, or otherwise does not necessarily constitute or imply its endorsement, recommendation, or favoring by the United States Government or any agency thereof. Their views and opinions of the authors expressed herein do

not necessarily state or reflect those of the United States Government or any agency thereof.

REFERENCES

[1] Musial W., and Ram B., 2010, "Large-scale offshore wind power in the United States: Assessment of opportunities and barriers", National Renewable Energy Laboratory (NREL), Golden, CO.

[2] Kunz T. H., Arnett E. B., Cooper B. M., Erickson W. P., Larkin R. P., Mabee T.,. Morrison M. L, Strickland M. D., and Szewczak J. M., 2007, "Assessing impacts of wind-energy development on nocturnally active birds and bats: A guidance document." Journal of Wildlife Management 71, pp. 2449-2486.

[3] Briggs, K. T., Tyler W. M. B., Lewis D. B., and Carlson D. R., 1987, "Bird communities at sea off California: 1975 to 1983," Studies in Avian Biology 11, pp. 1-74.

[4] Suryan, R. M., Phillips E. M., So K. J., Zamon J. E., Lowe R. W., and Stephensen S. W.. 2012, "Marine bird colony and at-sea distributions along the Oregon coast: Implications for marine spatial planning and information gap analysis," Oregon State University, Newport.

[5] Wiggelinkhuizen E., Rademakers L., Barhorst S., and Den Boon H., 2006, "Bird collision monitoring system for multi-megawatt wind turbines WT-Bird® Prototype development and testing."

[6] Desholm M., Fox A., Beasley P., and Kahlert J., 2006, "Remote techniques for counting and estimating the number of bird–wind turbine collisions at sea: a review," Ibis, 148(s1), pp. 76–89.

[7] Graps A., 1995, "An introduction to wavelets," Comput. Sci. Eng. IEEE, 2(2), pp. 50–61.

[8] Jiang Y., Tang B., Qin Y., and Liu W., 2011, "Feature extraction method of wind turbine based on adaptive Morlet wavelet and SVD," Renew. Energy, 36(8), pp. 2146–2153.

[9] Sung-Tae Park, and Jinguo Yang, 2004, "Engine knock detection based on wavelet transform," pp. 80–83 vol. 3.

[10] Vetterli M., and Herley C., 1992, "Wavelets and filter banks: theory and design," Signal Process. IEEE Trans. On, 40(9), pp. 2207–2232.

[11] Verhoef J. P., Westra C. A., Eecen P. J., Nijdam R. J., and Korterink H., 2003, "Development and first results of a bird impact detection system for wind turbines," ECN Wind Energy, Madrid, Spain.

[12] Grecian W. J., Inger R., Attrill M. J., Bearhop S., Godley B. J., Witt M. J., and Votier S. C., 2010, "Potential impacts of wave-powered marine renewable energy installations on marine birds," Ibis, 152(4), pp. 683–697.

[13] Boehlert G. W., and Gill A. B., 2010, "Environmental and ecological effects of ocean renewable energy development: a current synthesis," Oceanography 23, pp. 68-81

[14] Furness R. W., Wade H. M., Robbins A. M., and Masden E. A., 2012, "Assessing the sensitivity of seabird populations to adverse effects from tidal stream turbines and wave energy devices," ICES J. Mar. Sci. J. Cons., 69(8), pp. 1466–1479.

[15] Polagye, B., Copping A., Suryan R., Kramer S., Brown-Saracino J., and Smith C., 2014, "Instrumentation for monitoring around marine renewable energy converters: Workshop final report," PNNL-23110 Pacific Northwest National Laboratory, Seattle, Washington.

[16] Van Bussel G., and Zaaijer M., 2001, "Reliability, Availability and Maintenance aspects of large-scale offshore wind farms, a concepts study.," Newcastle, UK.

[17] Breton S.-P., and Moe G., 2009, "Status, plans and technologies for offshore wind turbines in Europe and North America," Renew. Energy, 34(3), pp. 646–654.

[18] Carbajo R. S., Staino A., Ryan K. P., Basu B., and Mc Goldrick C., 2011, "Characterisation of Wireless Sensor Platforms for Vibration Monitoring of Wind Turbine Blades."

[19] Swartz R. A., Lynch J. P., Sweetman B., Rolfes R., and Zerbst S., 2010, "Structural Monitoring of Wind Turbines using Wireless Sensor Networks," Smart Struct. Syst., 6(3), pp. 183–196.